Tracing star formation in giant molecular clouds: a spatially resolved study of NGC 253

Subhrata Dey

BP4, National Centre for Nuclear Research

NATIONAL CENTRE FOR NUCLEAR RESEARCH ŚWIERK

NATIONAL SCIENCE CENTRE POLAND

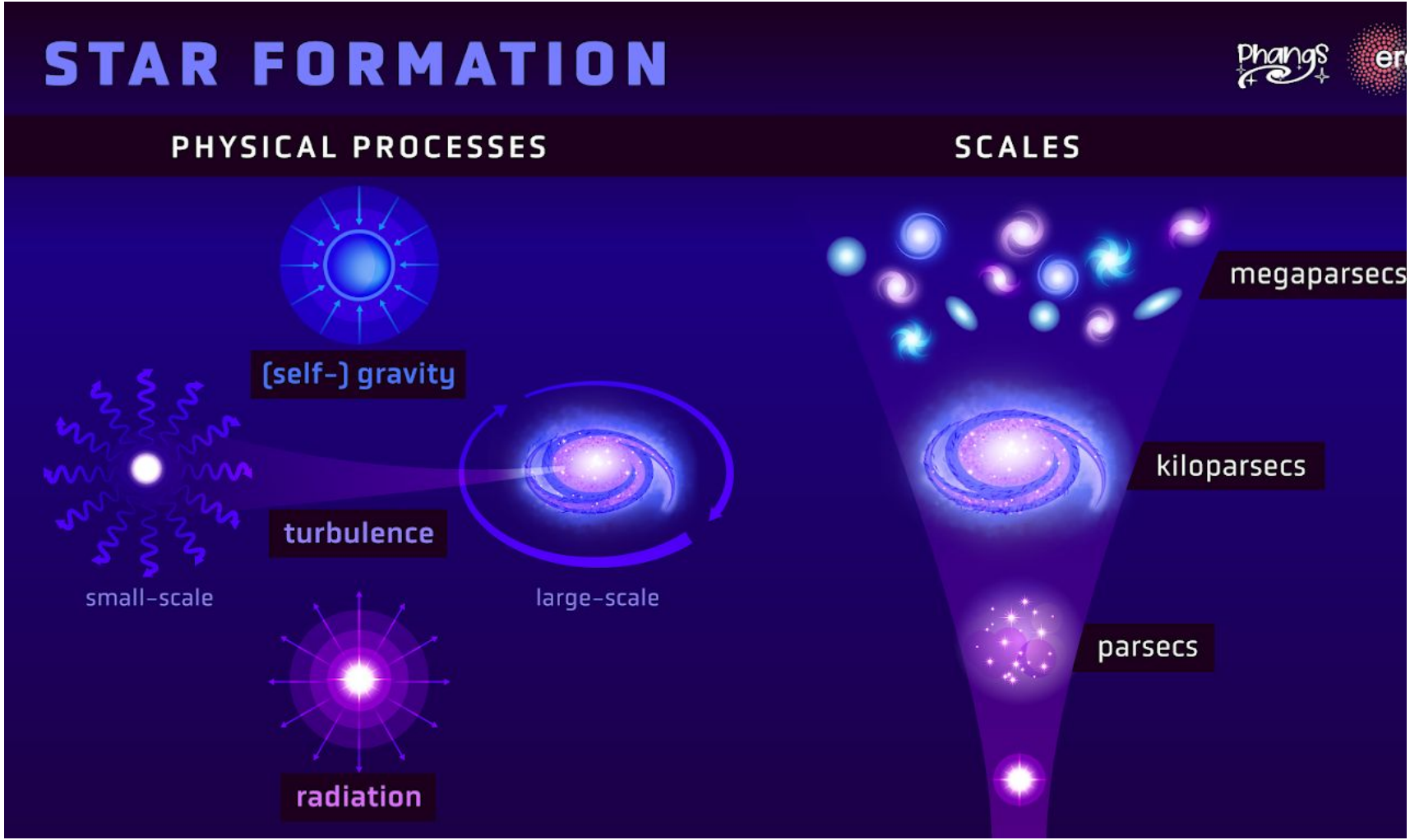
STAR FORMATION
PHYSICAL PROCESSES
SCALES
(self-) gravity
turbulence
radiation
small-scale
large-scale
megaparsecs
kiloparsecs
parsecs

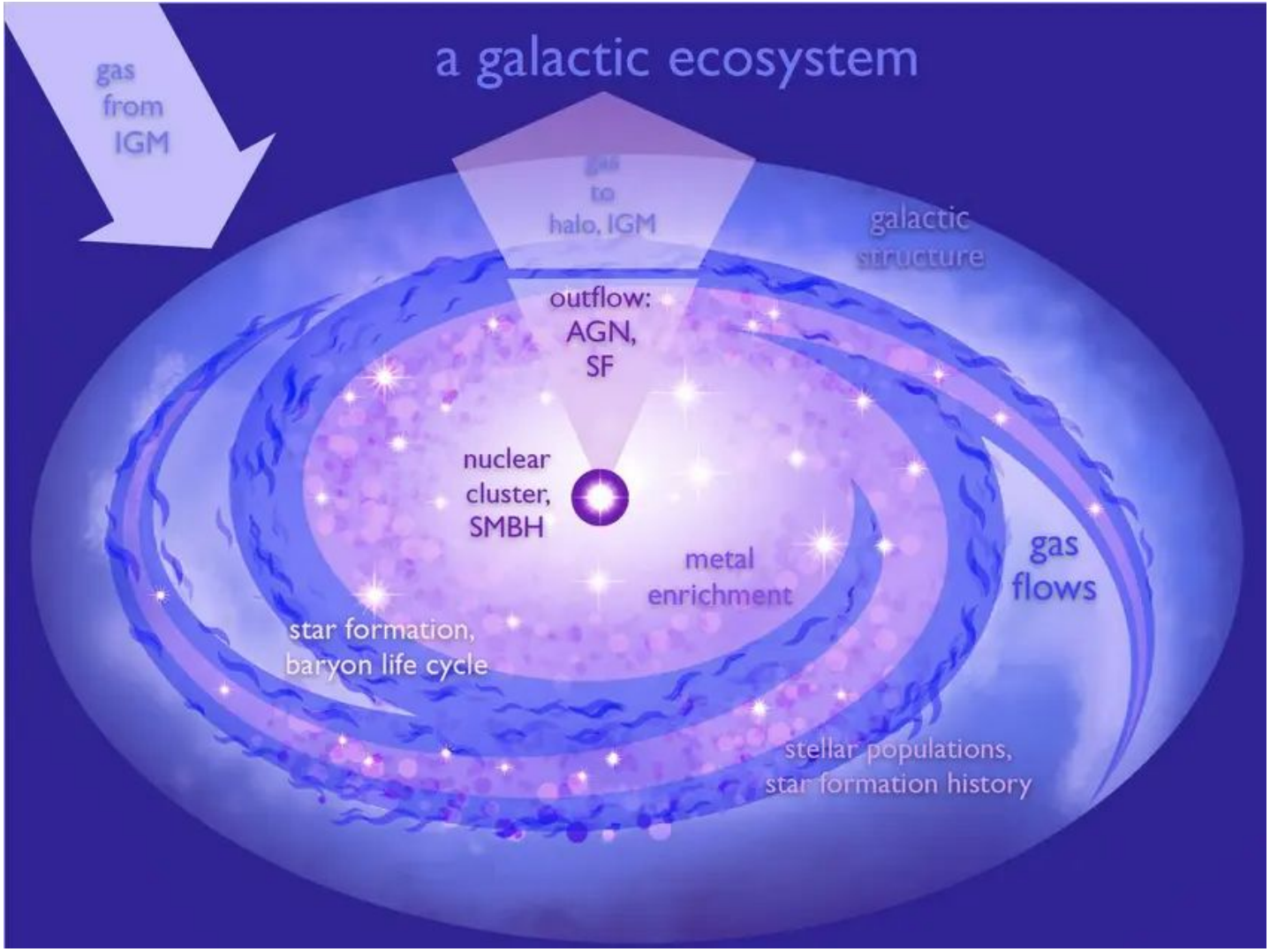
a galactic ecosystem
gas from IGM
gas to halo, IGM
galactic structure
outflow: AGN, SF
nuclear cluster, SMBH
metal enrichment
gas flows
star formation, baryon life cycle
stellar populations, star formation history

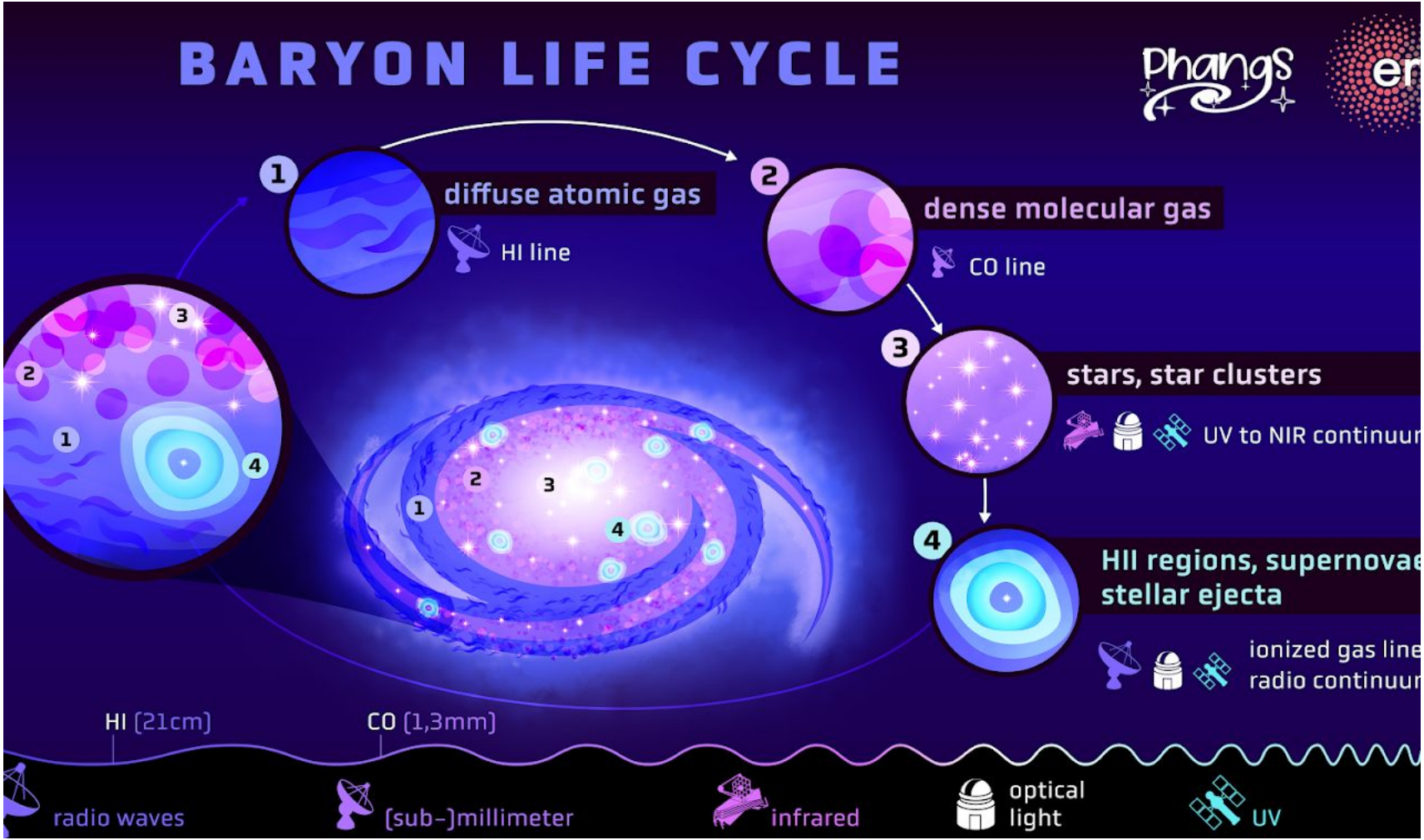
BARYON LIFE CYCLE
PHANGS
1
diffuse atomic gas
HI line
2
dense molecular gas
CO line
3
stars, star clusters
UV to NIR continuum
4
HII regions, supernovae
stellar ejecta
ionized gas line
radio continuum
HI (21cm)
CO (1,3mm)
radio waves
(sub-)millimeter
infrared
optical light
UV

NGC 253 (Sculpture galaxy)

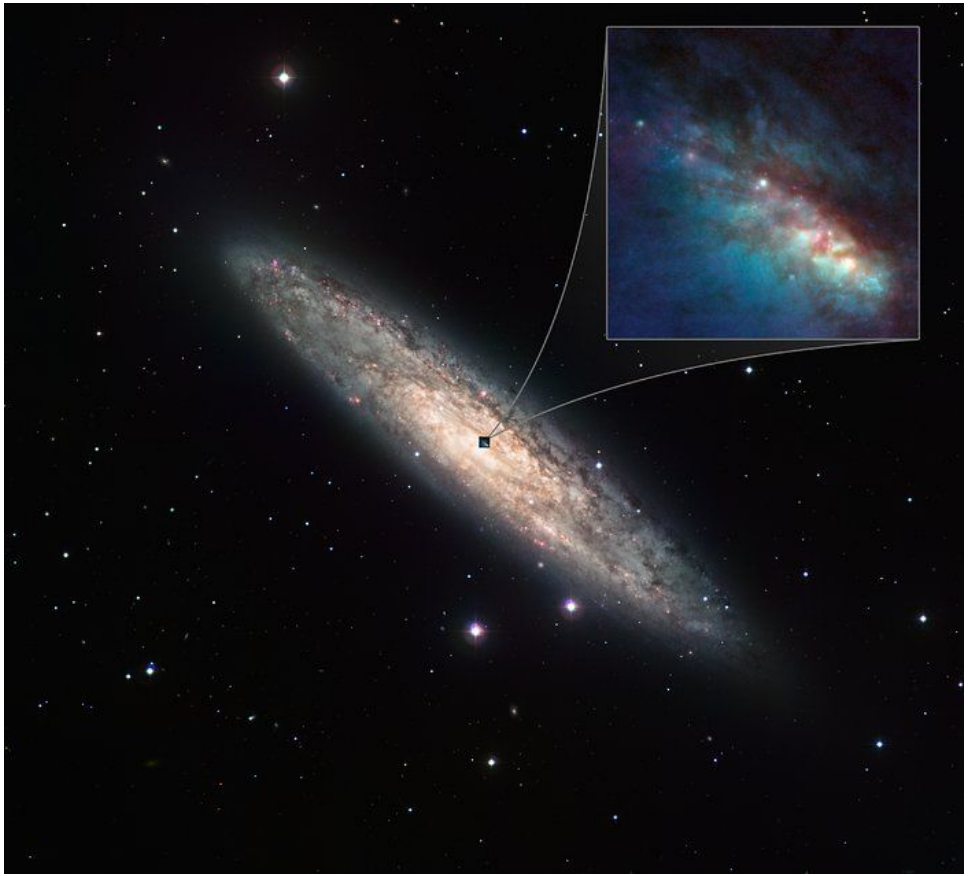

- ★ One of the nearest (~3.5 Mpc) and brightest starburst galaxies.
- ★ Nuclear star-formation rate is ~10–30× higher than in the Milky Way.
- ★ Central starburst hosts dense complexes of giant molecular clouds (GMCs).

NGC 253 (Sculpture galaxy)

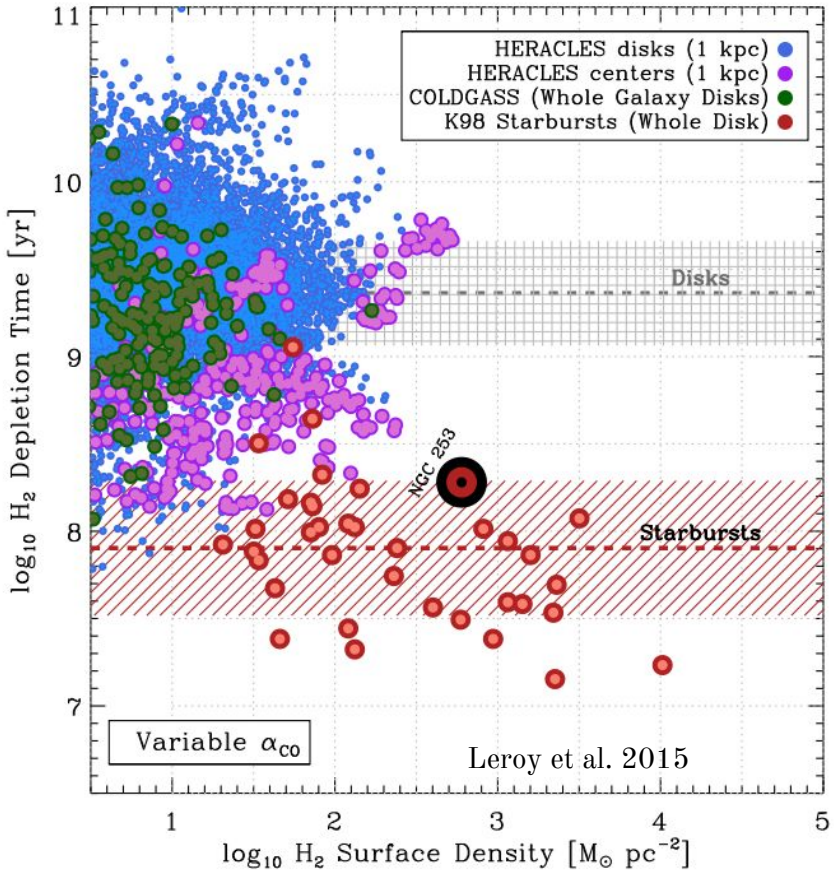

- ★ One of the nearest (~3.5 Mpc) and brightest starburst galaxies.
- ★ Nuclear star-formation rate is ~10–30× higher than in the Milky Way.
- ★ Central starburst hosts dense complexes of giant molecular clouds (GMCs).
- ★ **High gas surface densities:** Its central region reaches gas surface densities comparable to high-z submillimetre and extreme star-forming galaxies
- ★ **Short gas depletion times:** Like high-z galaxies (t_dep ~100–500 Myr), NGC 253's nuclear region consumes gas rapidly, much faster than typical local spirals.

Bridges our understanding between local star-forming environments and those in the early universe.




A&A, 699, A183 (2025)
https://doi.org/10.1051/0004-6361/202553897

Astronomy & Astrophysics

Spatially resolved spectrophotometric SED modeling of NGC 253's central molecular zone

I. Star formation in extragalactic giant molecular clouds

Pedro K. Humire[1,⋆], Subhrata Dey[2,3], Tommaso Ronconi[4,5,6,7], Victor H. Sasse[8], Roberto Cid Fernandes[8], Sergio Martín[9,10], Darko Donevski[3,4], Katarzyna Małek[3], Juan A. Fernández-Ontiveros[11], Yiqing Song[9,10], Mahmoud Hamed[3,12], Jeffrey G. Mangum[13], Christian Henkel[14,15], Víctor M. Rivilla[12], Laura Colzi[12], Nanase Harada[16,17,18], Ricardo Demarco[19], Arti Goyal[2], David S. Meier[20], Swayamtrupta Panda[21,⋆⋆], Ângela C. Krabbe[1], Yaoting Yan[14], Amanda R. Lopes[22], Kazushi Sakamoto[17], Sebastien Muller[23], Kunihiko Tanaka[24], Yuki Yoshimura[25], Kouichiro Nakanishi[16,18], Antonio Kanaan[8], Tiago Ribeiro[26], William Schoenell[27], and Claudia Mendes de Oliveira[1]

GMCs of NGC 253

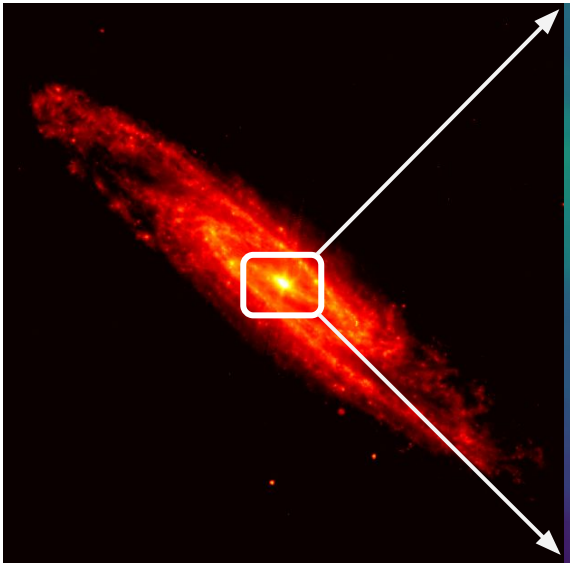

Gorski et al. 2017

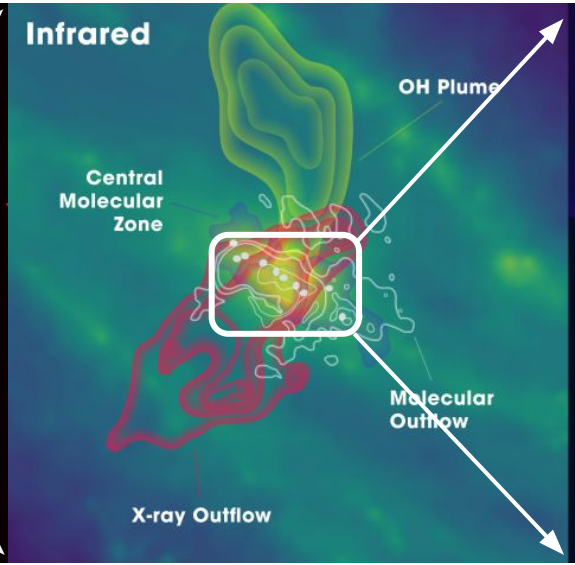

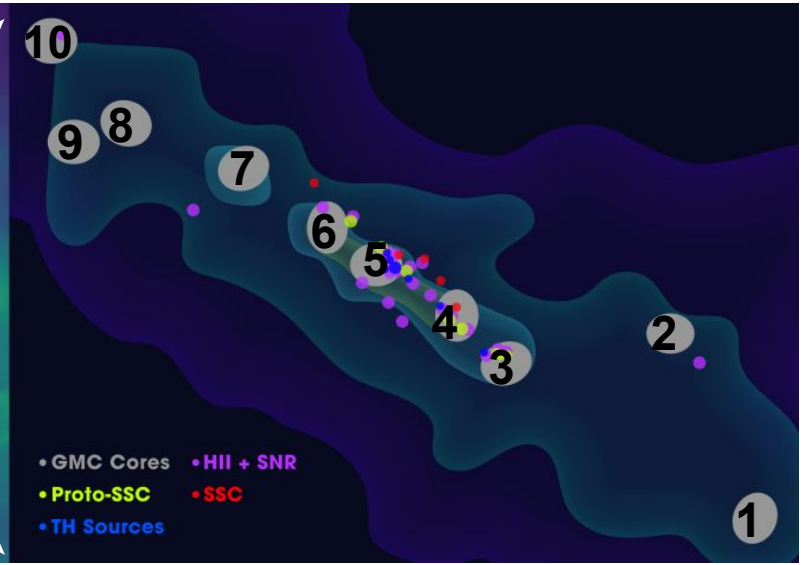

Martín et al. 2021

Literature: Wavelength specific studies

Optical

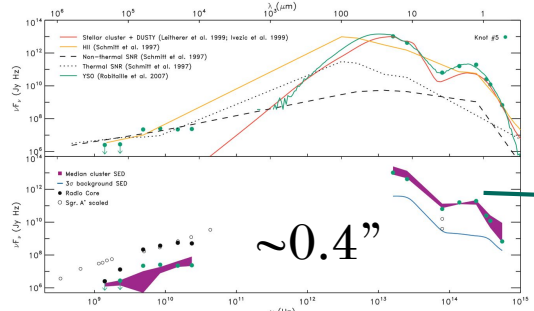

Fernández-Ontiveros+09

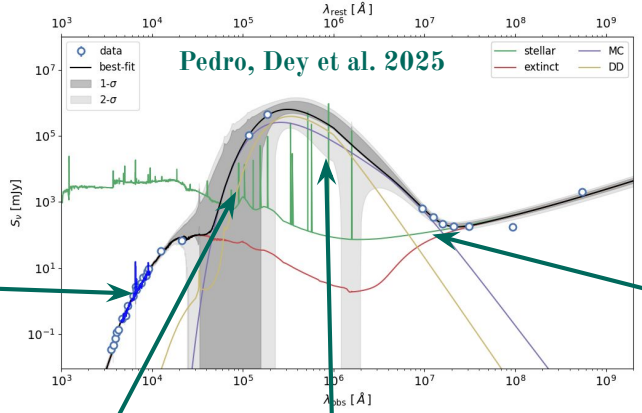

Sub-mm

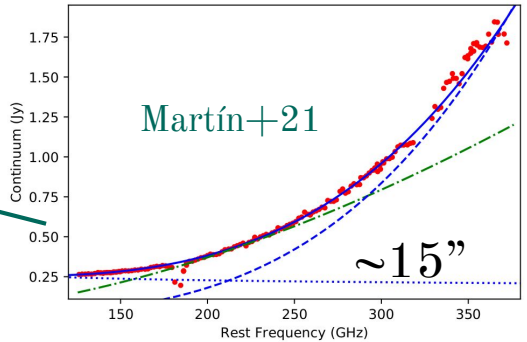

Optical + IR

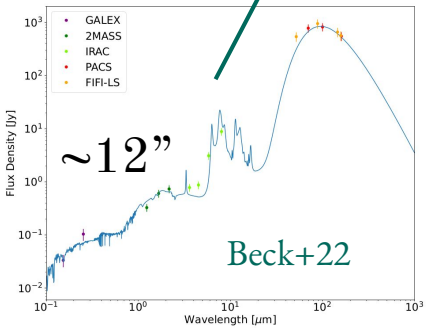

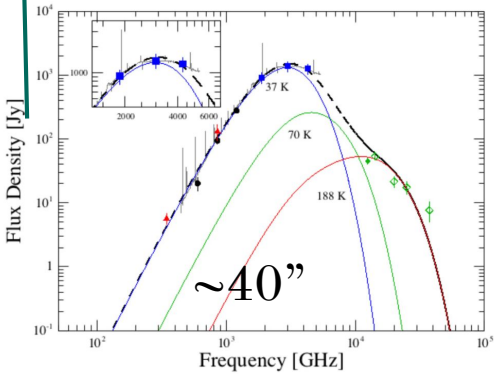

IR

Pérez-Beaupuits+18

Rich multiwavelength data

Band	Wavelength / Frequency	Instruments / Telescopes
Near-UV	3563 Å (uJAVA)	S-PLUS
Optical	3533–8941 Å (u, g, r, i, z)	S-PLUS
Optical	Hα, [O III], [S II], [N II] lines	VLT/MUSE
Optical	F555W, F658N, F814W	HST/ACS
NIR	J (1.265 μm), Ks (2.2 μm), L (3.8 μm), Brα	VLT/NaCo (adaptive optics)
MIR	3.6, 4.5, 5.8, 8.0 μm	Spitzer/IRAC
MIR	8.6 μm (PAH2), 11.9 μm (N), 18.72 μm (Qa)	VLT/VISIR
FIR	70 μm, 100 μm, 160 μm	Herschel/PACS
Submm/mm	0.8–3.6 mm (84–373 GHz, ALMA Bands 3–7)	ALMA
Radio	1.5 GHz, 5.5 GHz, 10 GHz, 33 GHz, 91 GHz	VLA / EVLA
Radio Recombination Lines	H40α (99 GHz), H41α, H52α, etc.	VLA / EVLA

GMC fluxes extracted using uniform 3″ (~50 pc) apertures at positions to ensure consistent physical scales across all bands.

First *UV to radio* panchromatic SED study of a spatially resolved galaxy!!

Panchromatic spectral energy distribution (SED)

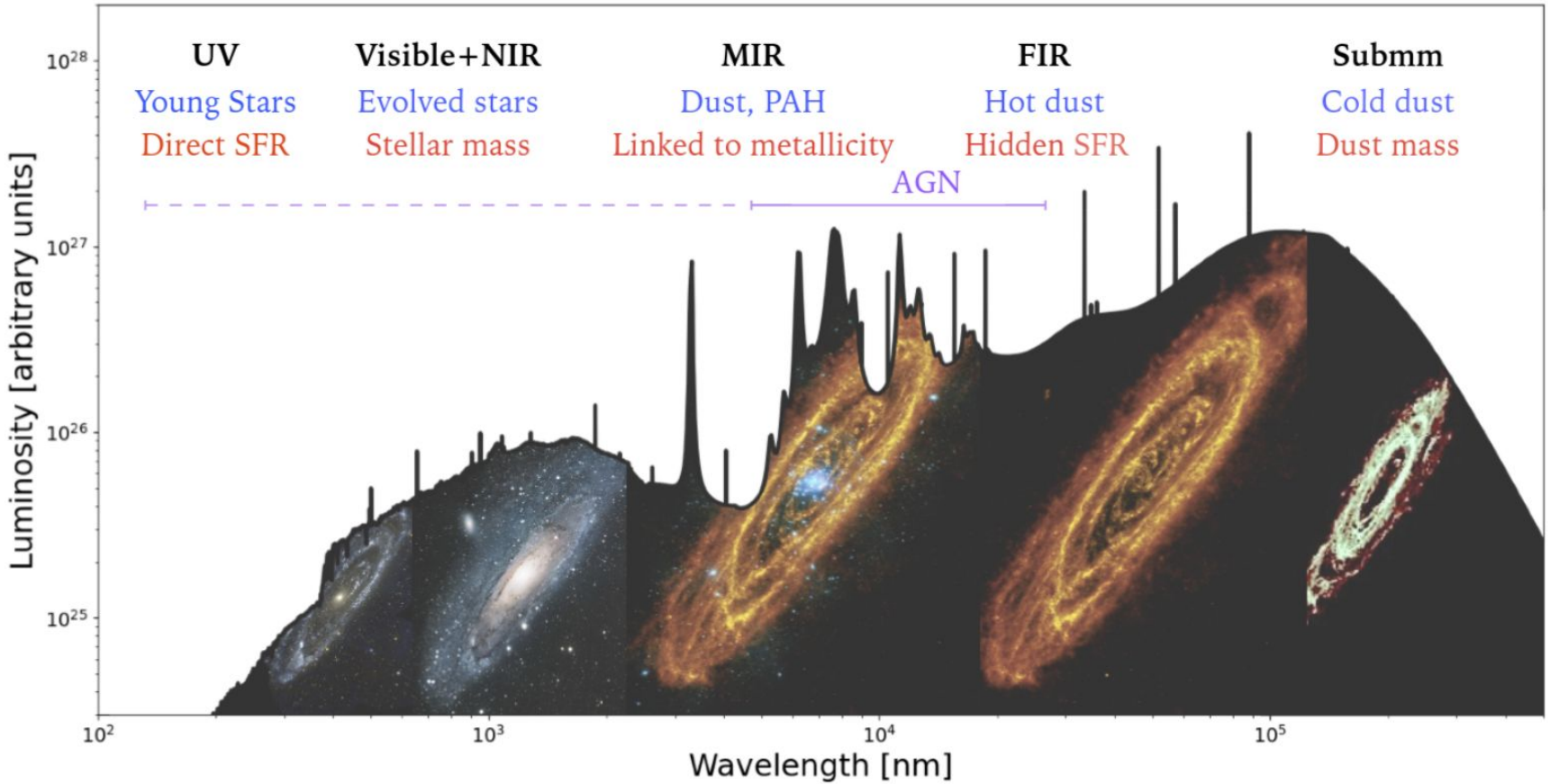

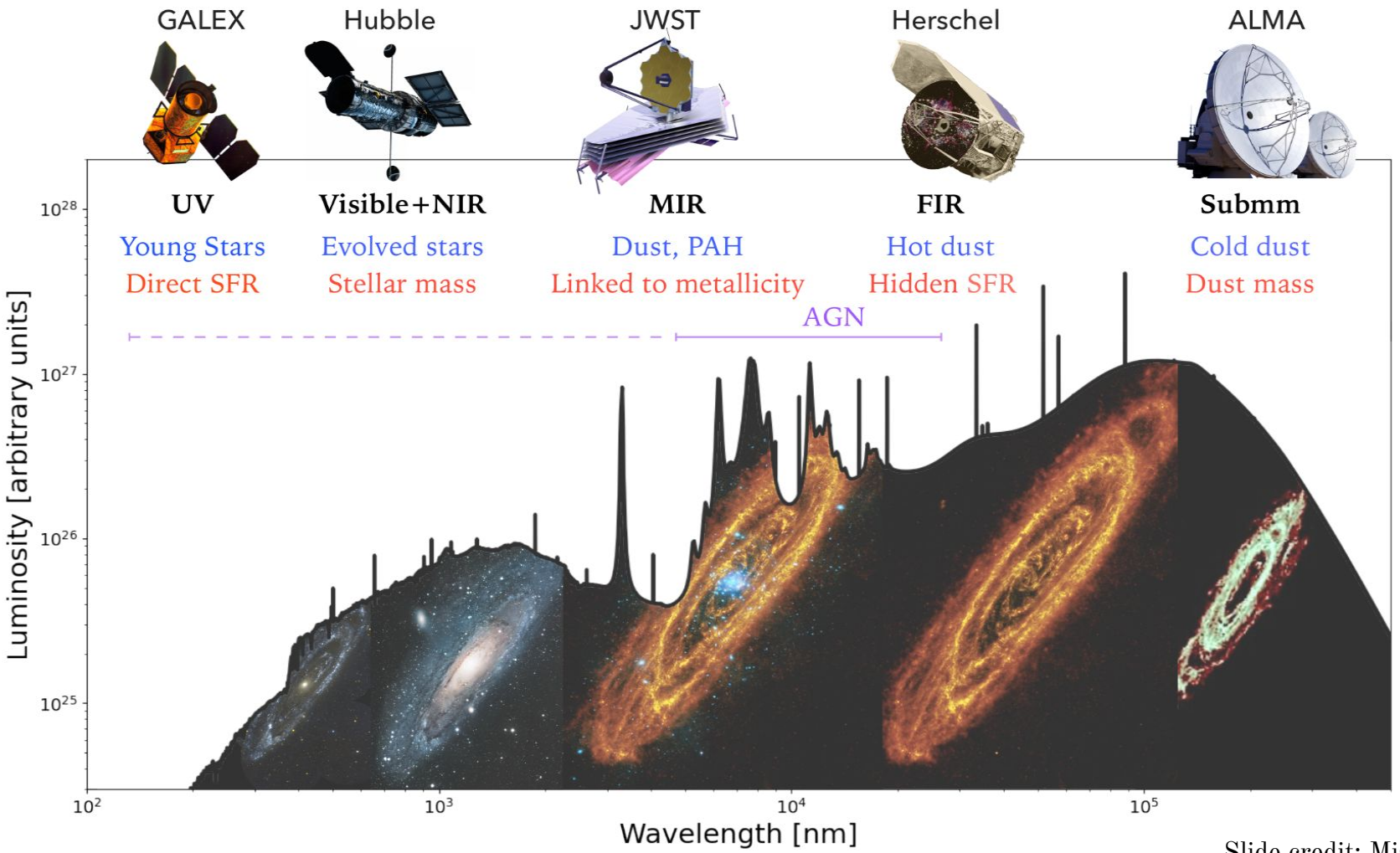

Slide credit: Misa Hamed

Analysis: SED modeling

A&A, 685, A161 (2024)
https://doi.org/10.1051/0004-6361/202346978

Astronomy & Astrophysics

GalaPy: A highly optimised C++/Python spectral modelling tool for galaxies

I. Library presentation and photometric fitting

T. Ronconi[1,2,3,11], A. Lapi[1,2,4,5], M. Torsello[1], A. Bressan[1], D. Donevski[6,1], L. Pantoni[7], M. Behiri[1], L. Boco[1], A. Cimatti[8], Q. D'Amato[9], L. Danese[1], M. Giulietti[1], F. Perrotta[1], L. Silva[10], M. Talia[8], and M. Massardi[4,1]

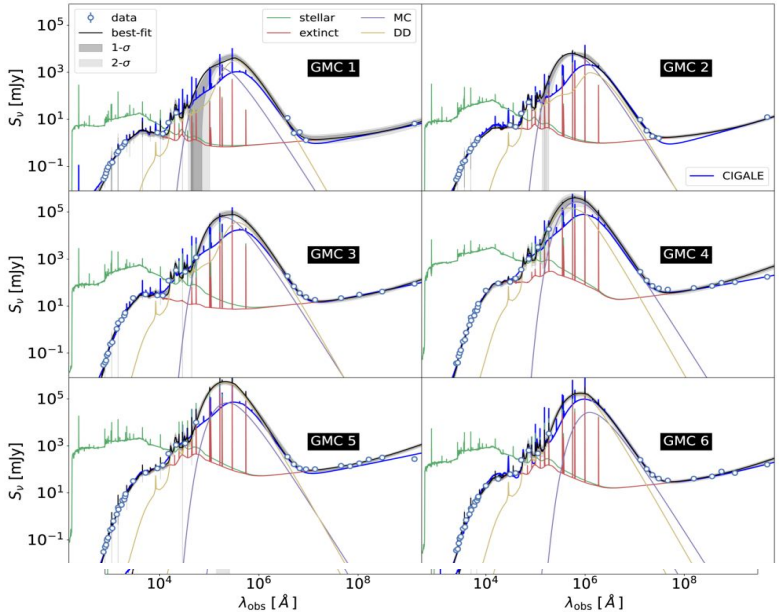

Analysis: SED modeling

A&A, 685, A161 (2024)
https://doi.org/10.1051/0004-6361/202346978

Astronomy & Astrophysics

GalaPy: A highly optimised C++/Python spectral modelling tool for galaxies

I. Library presentation and photometric fitting

T. Ronconi[1,2,3,11], A. Lapi[1,2,4,5], M. Torsello[1], A. Bressan[1], D. Donevski[6,1], L. Pantoni[7], M. Behiri[1], L. Boco[1], A. Cimatti[8], Q. D'Amato[9], L. Danese[1], M. Giulietti[1], F. Perrotta[1], L. Silva[10], M. Talia[8], and M. Massardi[4,1]

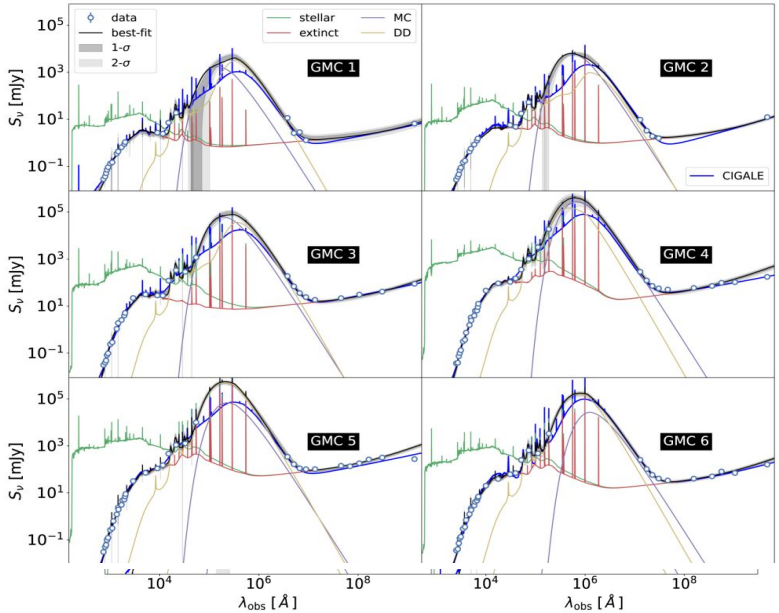

A&A 622, A103 (2019)
https://doi.org/10.1051/0004-6361/201834156

Astronomy & Astrophysics

CIGALE: a python Code Investigating GALaxy Emission★

M. Boquien[1], D. Burgarella[2], Y. Roehlly[2], V. Buat[2], L. Ciesla[2], D. Corre[2], A. K. Inoue (井上昭雄)[3], and H. Salas[1]

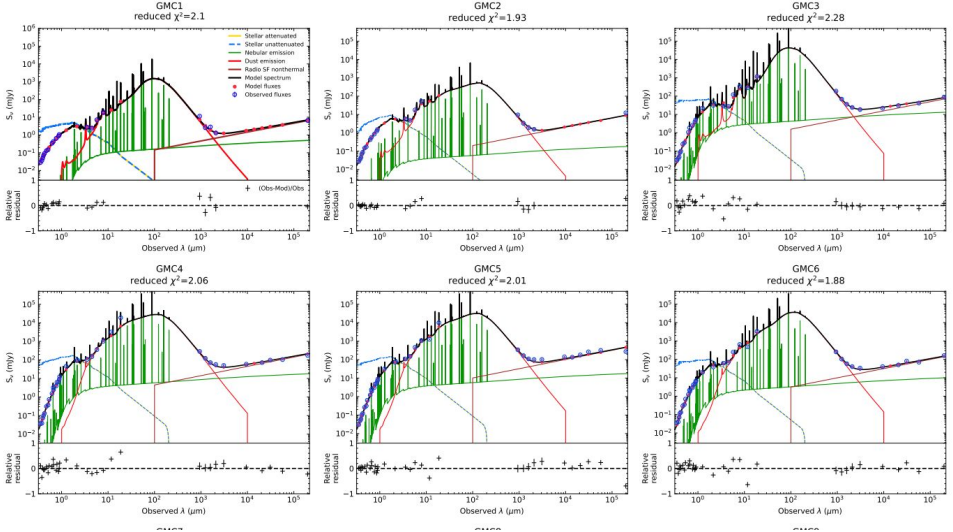

Analysis: SED modeling

A&A, 685, A161 (2024)
https://doi.org/10.1051/0004-6361/202346978

Astronomy & Astrophysics

GalaPy: A highly optimised C++/Python spectral modelling tool for galaxies

I. Library presentation and photometric fitting

T. Ronconi[1,2,3,11], A. Lapi[1,2,4,5], M. Torsello[1], A. Bressan[1], D. Donevski[6,1], L. Pantoni[7], M. Behiri[1], L. Boco[1], A. Cimatti[8], Q. D'Amato[9], L. Danese[1], M. Giulietti[1], F. Perrotta[1], L. Silva[10], M. Talia[8], and M. Massardi[4,1]

A&A 622, A103 (2019)
https://doi.org/10.1051/0004-6361/201834156

Astronomy & Astrophysics

CIGALE: a python Code Investigating GALaxy Emission★

M. Boquien[1], D. Burgarella[2], Y. Roehlly[2], V. Buat[2], L. Ciesla[2], D. Corre[2], A. K. Inoue (井上昭雄)[3], and H. Salas[1]

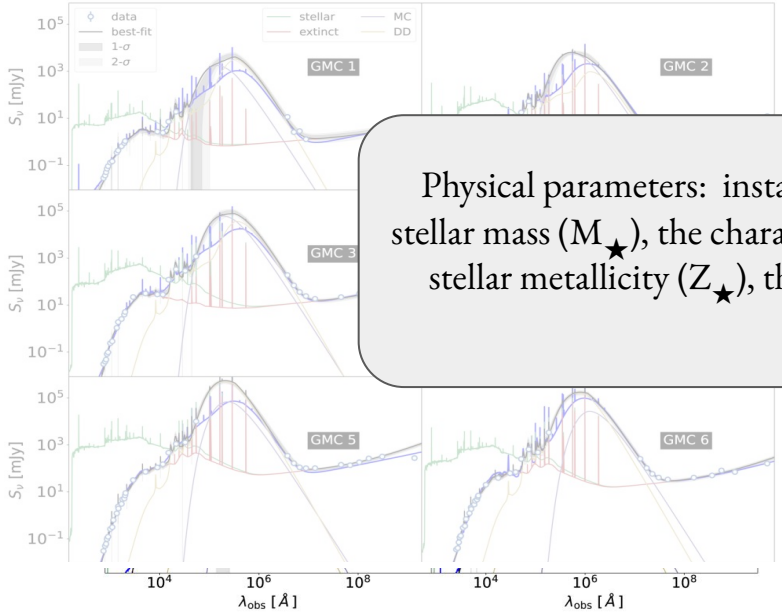

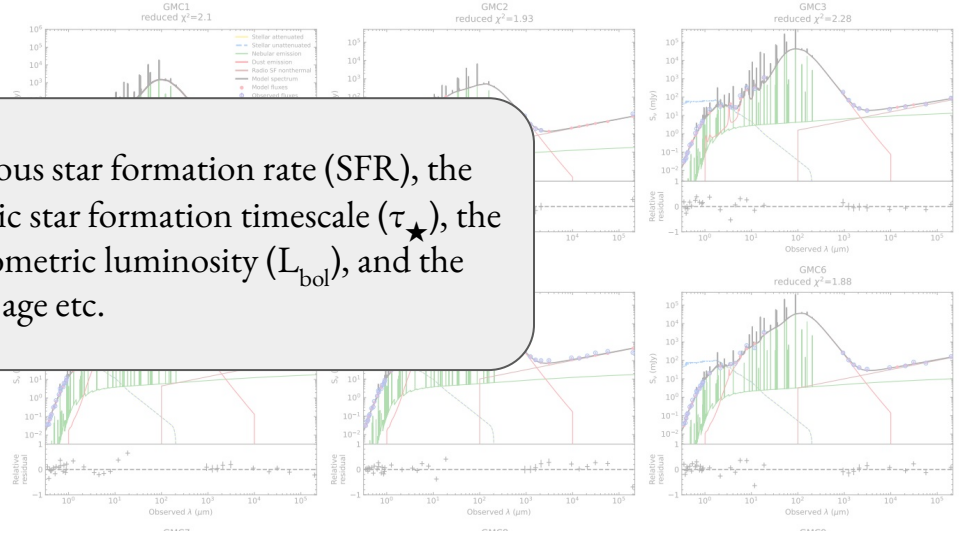

Physical parameters: instantaneous star formation rate (SFR), the stellar mass ($M_\star$), the characteristic star formation timescale ($\tau_\star$), the stellar metallicity ($Z_\star$), the bolometric luminosity (L_{bol}), and the stellar age etc.

Analysis: Optical spectra modeling

STARLIGHT (Cid Fernandes et al. 2005)

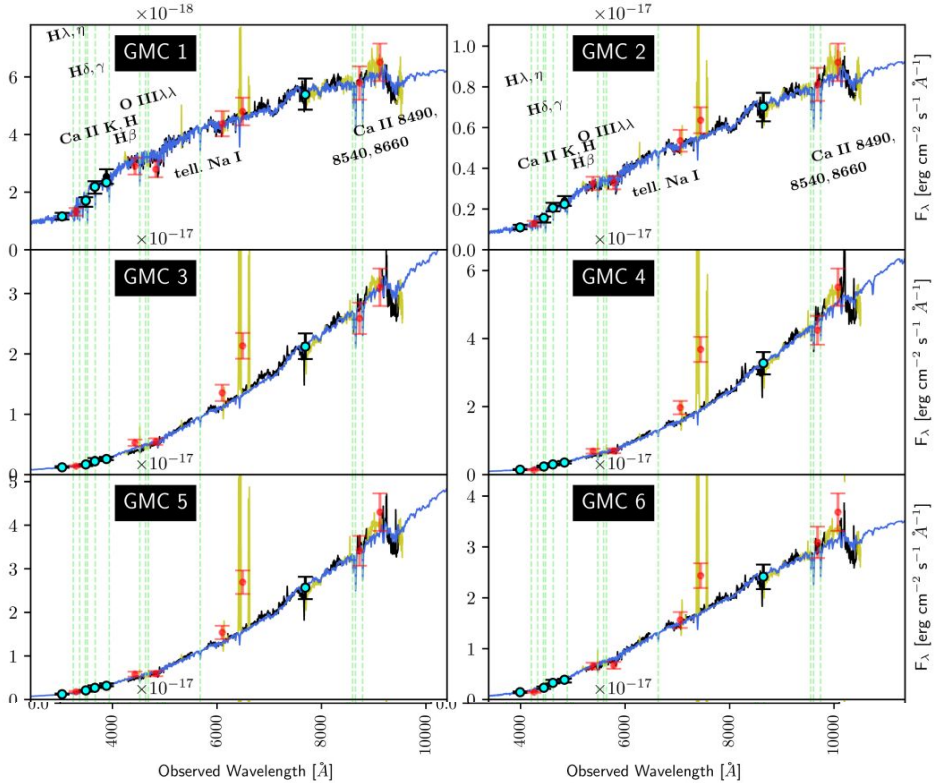

Analysis: Optical spectra modeling

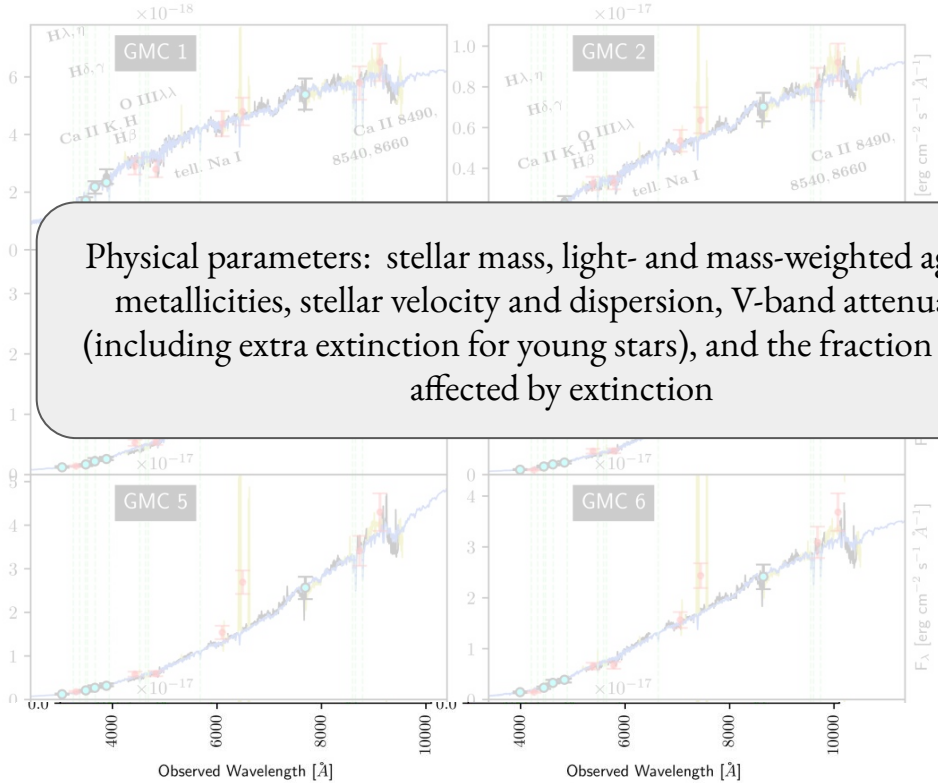

Physical parameters: stellar mass, light- and mass-weighted ages and metallicities, stellar velocity and dispersion, V-band attenuation (including extra extinction for young stars), and the fraction of stars affected by extinction

GMC characteristics

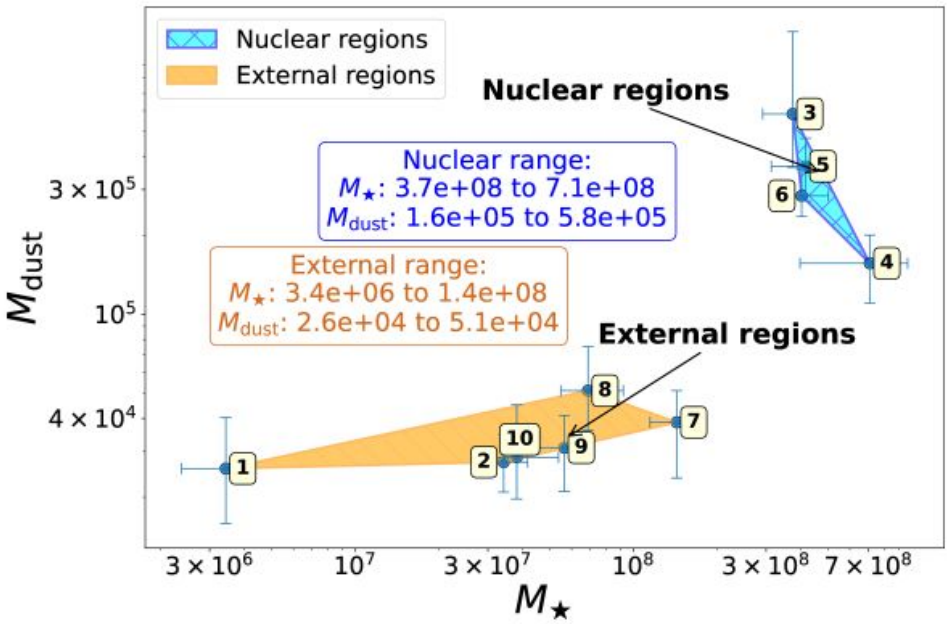

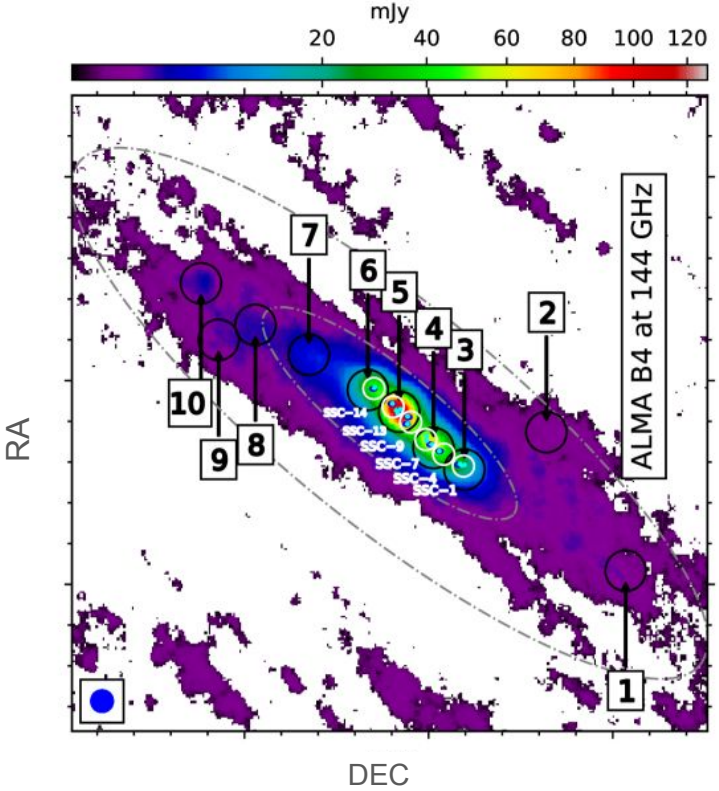

GMC characteristics

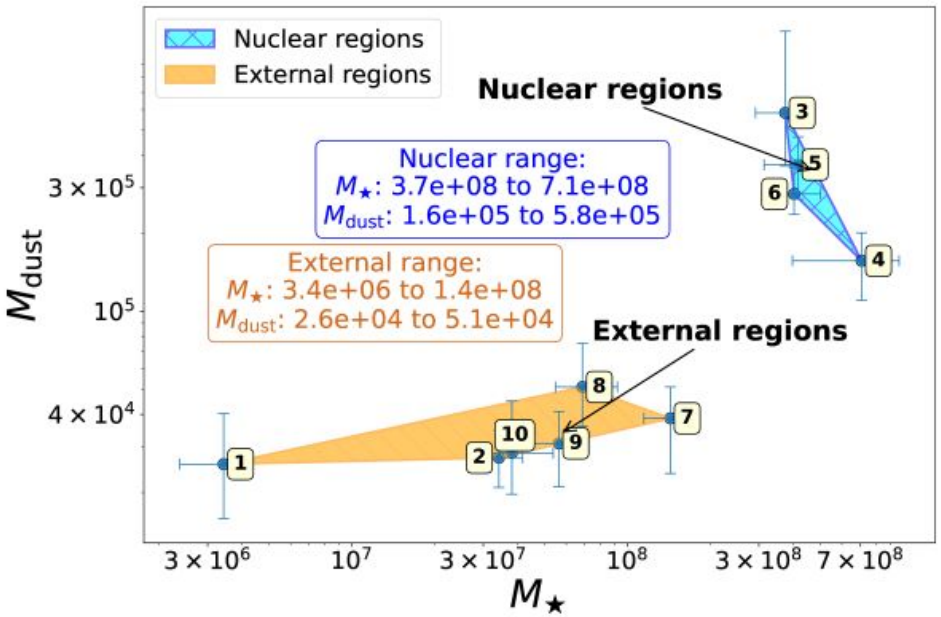

Internal GMCs (3–6) : central ~120 pc, **high SFR** ($\gtrsim$0.087 $M_\odot$ yr^{-1}), **large dust masses** , fast shocks from intense star formation.

External GMCs (1, 2, 7–10) : periphery, **low SFR** (0.005–0.022 $M_\odot$ yr^{-1}), **smaller dust masses** , slower shocks dominate chemistry.

SFR and dust content closely reflect the physical environment and location within the CMZ.

Emission line diagnostic diagrams

WHAN diagram

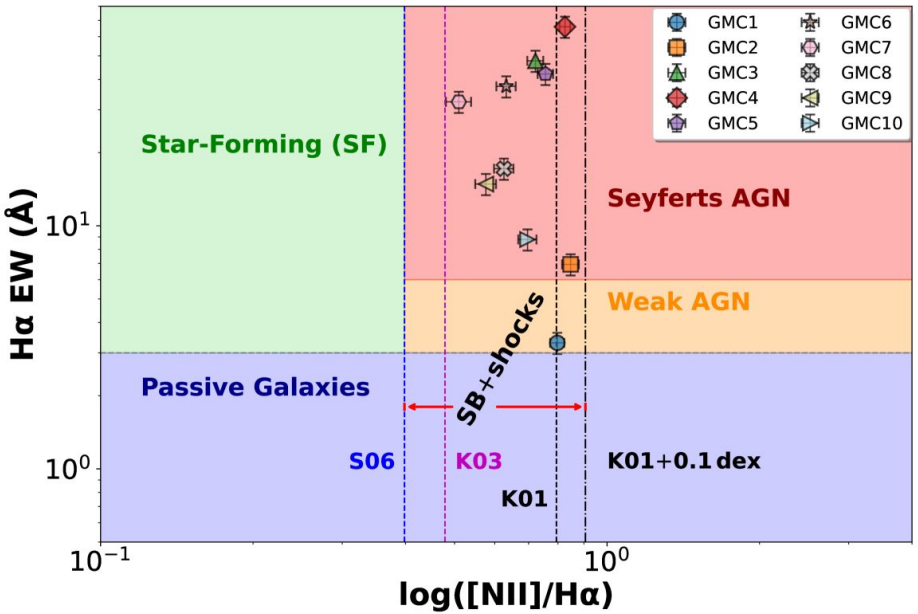

BPT diagram

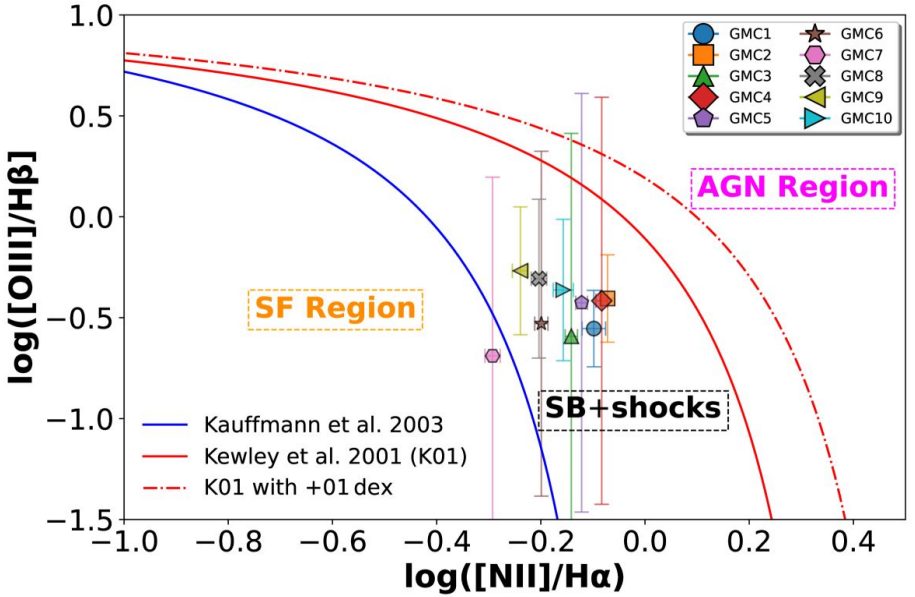

★ **"Starburst + shocks" composites** => line ratios reflecting **star formation and shocks** from stellar winds and supernovae.

★ **SED analysis =>AGN fraction is negligible (<7.5%)**

Star formation rates (SFR)

Kennicutt (1998): Hα–SFR calibration

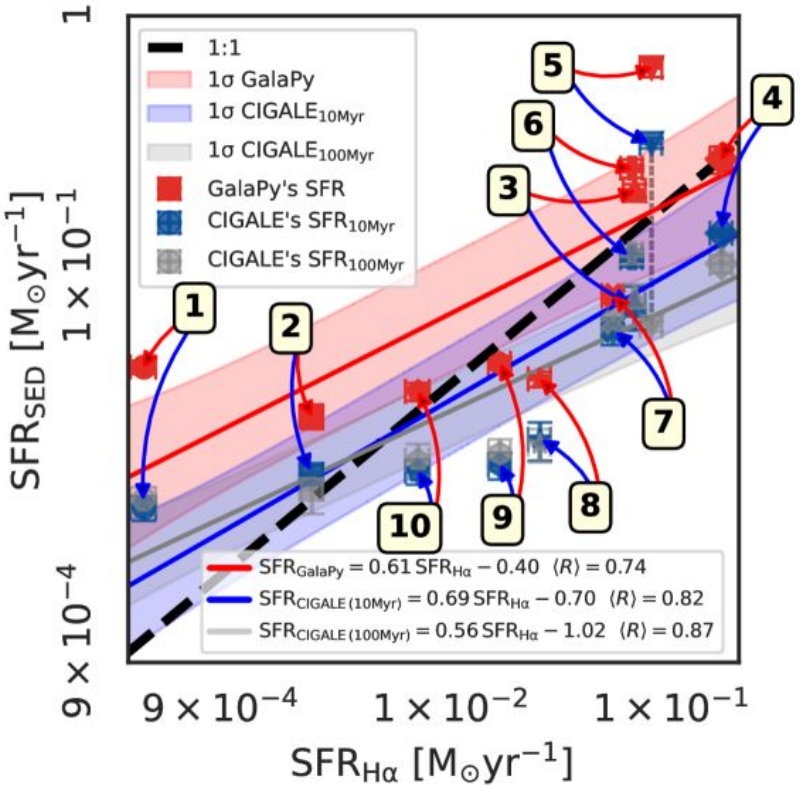

Kennicutt relation (Kennicutt 1998)

$$\mathrm{SFR}\ [\mathrm{M_\odot\ year^{-1}}] = 7.9 \times 10^{-42} \mathrm{L}(\mathrm{H}\alpha)\ [\mathrm{erg\ s^{-1}}].$$

Star formation rates (SFR)

Kennicutt (1998): Hα–SFR calibration

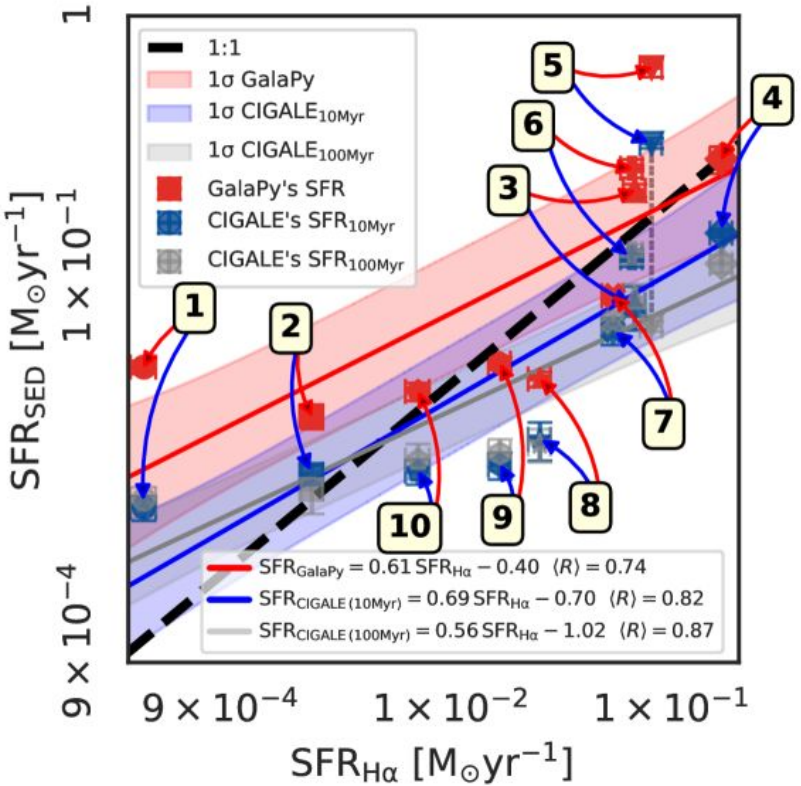

Kennicutt relation (Kennicutt 1998)

$$\mathrm{SFR}\ [\mathrm{M_\odot\ year^{-1}}] = 7.9 \times 10^{-42} \mathrm{L}(\mathrm{H}\alpha)\ [\mathrm{erg\ s^{-1}}].$$

GalaPy SFRs (red points) are higher than Kennicutt => instantaneous SFR (Galapy, ***captures recent burst***) > average SFR over 10 Myr (traced by Hα)

CIGALE SFRs averaged over 10 Myr (blue) slope closer to 1
=> Consistent with the timescale Hα probes SFR expectations.

Star formation rates (SFR)

Radio emission: Extinction free!!

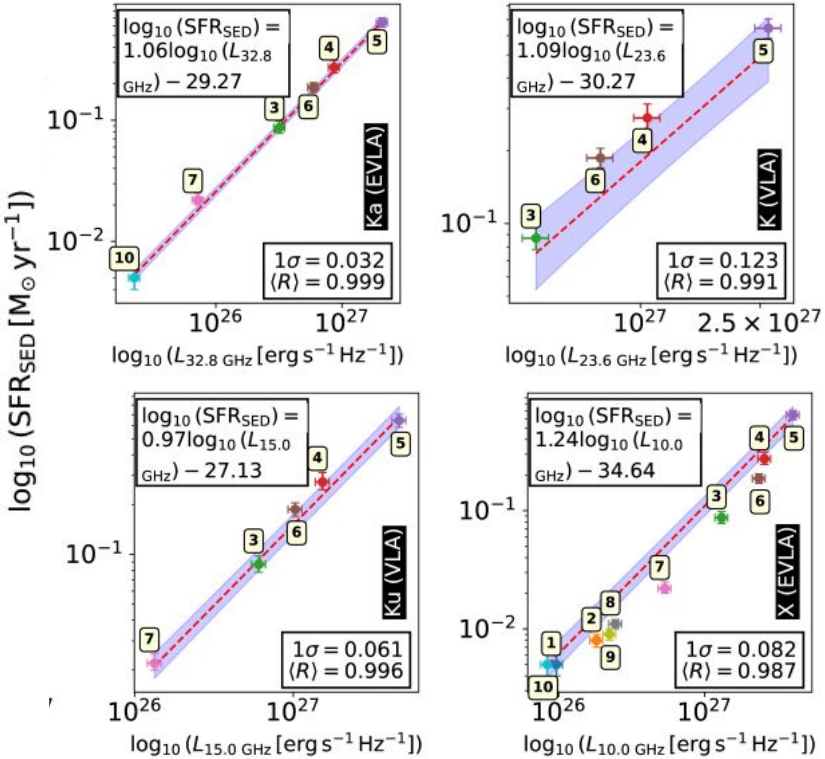

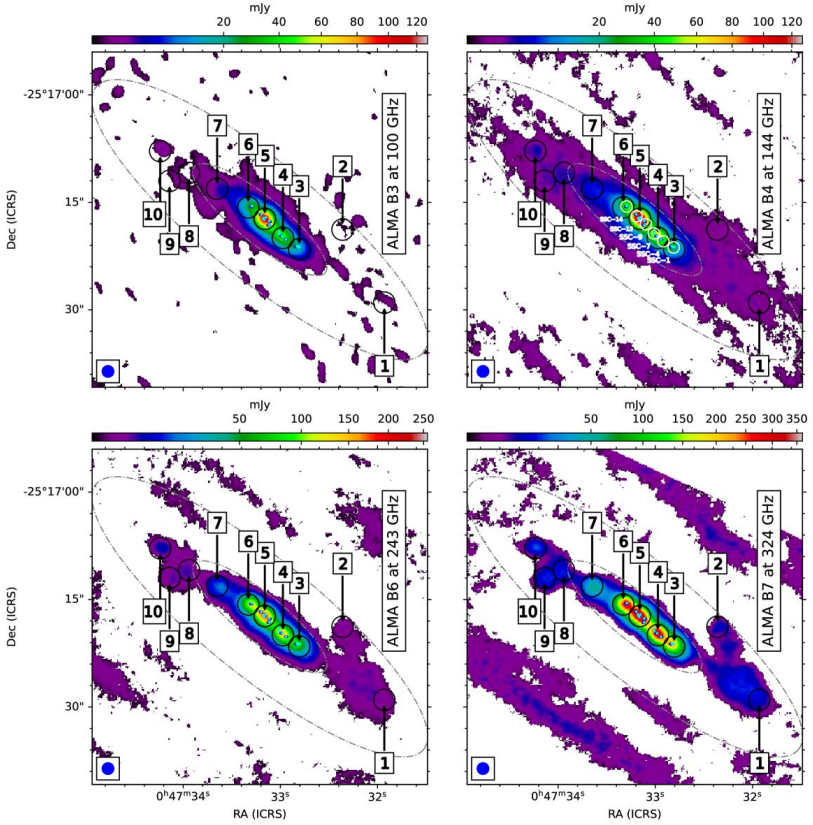

Star formation rates (SFR)

Radio emission: Extinction free!!

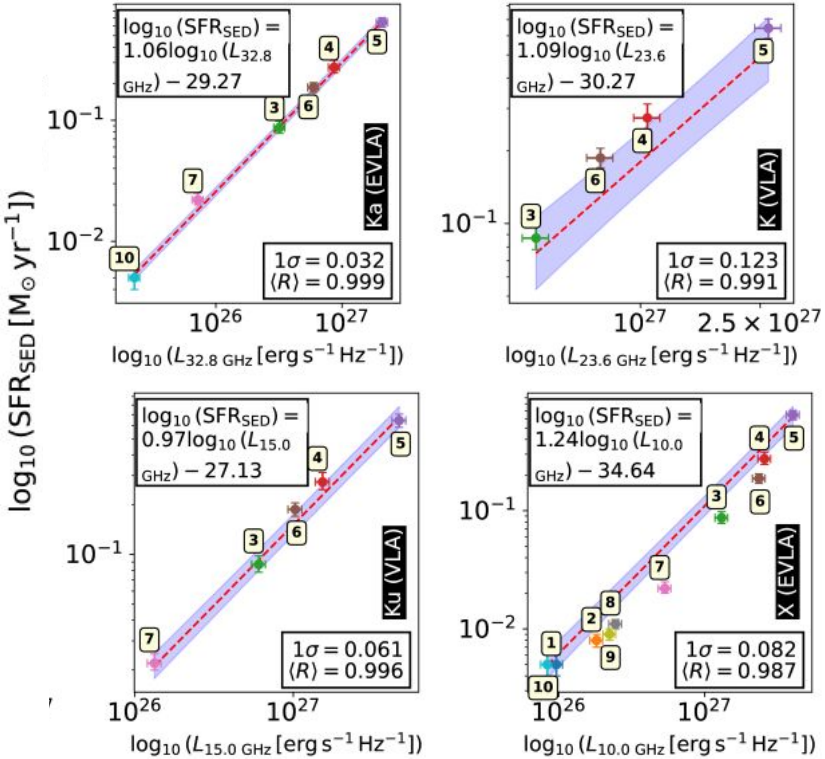

★ *Radio emission effectively traces star formation in highly obscured GMCs*

★ Multiple radio continuum bands correlates SED-derived SFRs, even in regions where dust obscures traditional tracers.

★ Strong correlation between radio luminosity and SED SFRs demonstrates that SED modeling accurately captures obscured star formation.

Star formation rates (SFR)

Radio emission: Extinction free!!

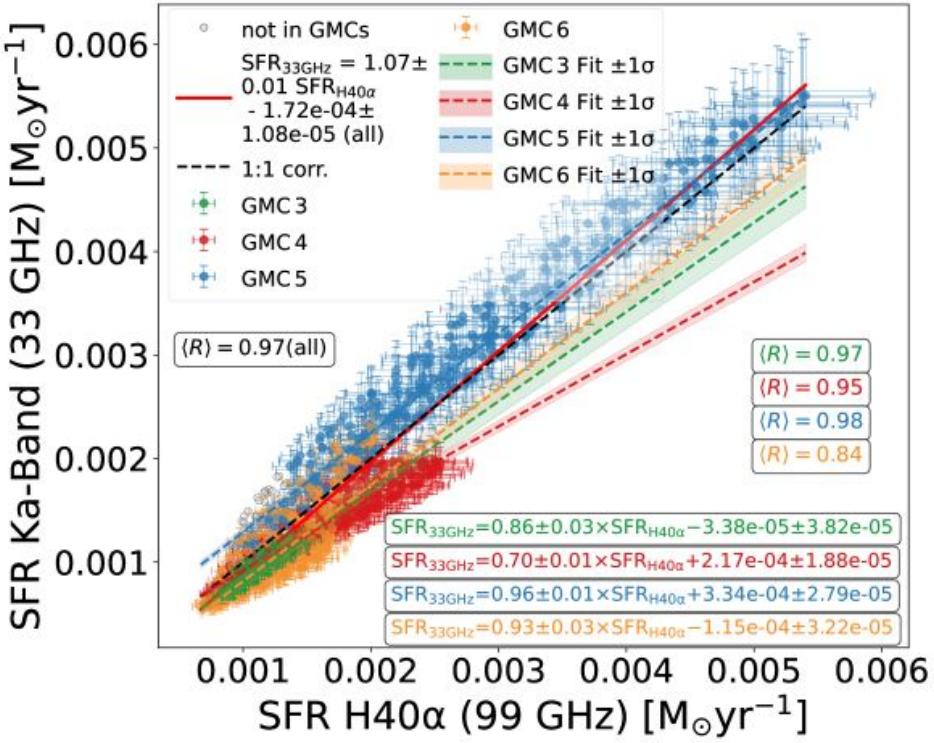

Star formation rates (SFR)

Radio emission: Extinction free!!

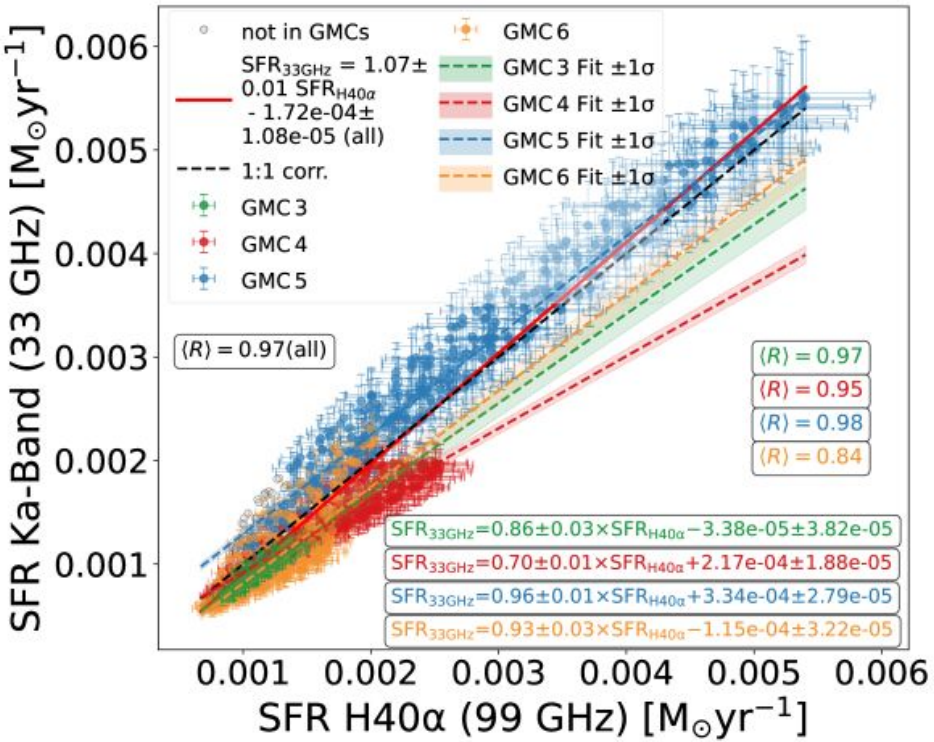

★ **Ka-band (~33 GHz):** Free–free emission → traces current star formation.

★ **H40α (~99 GHz):** Measures ionizing photon rate → independent SFR tracer.

★ SFRs from both tracers agree well!!
★ Reliable in dense, obscured GMCs.

Comparison with high-z dusty starbursts

Property	NGC 253 GMCs	High-z Dusty Starbursts	References
Dust-to-stellar mass ratio (log $M_{dust}/M_{\star}$)	−2.32 ± 0.29 (CIGALE)	−2.13 ± 0.3 (z ≈ 2–5)	Donevski+20
Dust-to-stellar mass ratio (log $M_{dust}/M_{\star}$)	−2.89 ± 0.45 (GalaPy)	−2.58 ± 0.4 (z ≈ 4–6)	Sawant+25
Attenuation	High; similar to dusty starbursts	High; strongly obscured	Nanni+20; Álvarez-Márquez+23
Stellar mass ($M_{\star}$)	Low (10^4–10^8 $M_{\odot}$)	Very high (10^9–10^{11} $M_{\odot}$)	Sawant+25
SFR	Low (0.005–0.1 $M_{\odot}$/yr)	High (10–1000 $M_{\odot}$/yr)	Salak+24
SFR-to-stellar mass ratio (sSFR)	Low	Very high	Donevski+20
Dominant dust source	Type II SNe + possible ISM grain growth	Rapid dust growth + stellar sources	Hirashita & Chen 23; Palla+24
Outflows	Strong, may enhance grain growth	Strong in many high-z systems	Narayanan+25

Conclusions

★ First 51-pc *UV–to–radio* panchromatic SED study of NGC 253's CMZ

★ Nuclear vs. external GMCs**:** *Internal clouds* (GMCs 3–6) show higher dust/stellar masses, sSFRs, excitation, and stronger shocks, reflecting *intense star formation*; external clouds are less dense and less active.

★ **Emission-line diagnostics (BPT/WHAN)** indicate shock-driven ionization from stellar feedback, not AGN activity.

★ **SFR tracers:** *33 GHz (radio!!) Ka-band continuum correlates tightly with SED-derived SFRs; Hα (optical) underestimates SFR; RRLs (H40α) effective only for brightest GMCs.*

★ **NGC 253 as a local laboratory to study high-z starbursts:** GMCs reproduce dust-to-stellar mass ratios and attenuation seen in $z \simeq 2$–6 dusty galaxies, providing a nearby platform to study feedback, dust growth, and starburst physics.

Dziękuję!!

Table 5. GalaPy results for star-formation-related properties.

GMC	SFR $[\times 10^{-4} M_\odot\ \mathrm{yr}^{-1}]$	$M_\star$ $[\log_{10}(M_\odot)]$	$\tau_\star$ $[\log_{10}(\mathrm{yr})]$	$Z_\star$ $[\times 10^{-3}]$	L_{bol} $[\log_{10}(L_\odot)]$	Age $[\log_{10}(\mathrm{yr})]$
1	50^{+10}_{-10}	$6.535^{+0.159}_{-0.097}$	$10.88^{+0.08}_{-0.21}$	$0.35^{+0.18}_{-0.08}$	$8.065^{+0.052}_{-0.073}$	$9.30^{+0.15}_{-0.13}$
2	80^{+10}_{-10}	$7.534^{+0.106}_{-0.086}$	$9.21^{+0.14}_{-0.14}$	$3.88^{+0.19}_{-0.15}$	$8.391^{+-0.002}_{-0.062}$	$9.66^{+0.13}_{-0.12}$
3	870^{+110}_{-90}	$8.573^{+0.108}_{-0.100}$	$9.07^{+0.28}_{-0.46}$	$7.88^{+2.27}_{-0.94}$	$9.354^{+0.071}_{-0.042}$	$9.62^{+0.15}_{-0.23}$
4	2740^{+390}_{-280}	$8.850^{+0.251}_{-0.136}$	$7.48^{+0.13}_{-0.10}$	$20.84^{+2.31}_{-1.47}$	$10.132^{+0.050}_{-0.114}$	$8.54^{+0.16}_{-0.08}$
5	6450^{+600}_{-590}	$8.620^{+0.124}_{-0.105}$	$7.57^{+0.12}_{-0.11}$	$17.59^{+1.17}_{-1.14}$	$10.184^{+0.016}_{-0.065}$	$8.40^{+0.13}_{-0.03}$
6	1870^{+180}_{-170}	$8.605^{+0.072}_{-0.095}$	$8.17^{+0.10}_{-0.12}$	$12.87^{+0.82}_{-0.63}$	$9.602^{+0.061}_{-0.045}$	$8.56^{+0.06}_{-0.04}$
7	220^{+30}_{-20}	$8.156^{+0.096}_{-0.087}$	$8.50^{+0.31}_{-0.18}$	$8.12^{+0.87}_{-1.18}$	$8.903^{+0.041}_{-0.080}$	$9.39^{+0.23}_{-0.14}$
8	110^{+10}_{-10}	$7.837^{+0.098}_{-0.127}$	$9.24^{+0.24}_{-0.24}$	$4.45^{+0.71}_{-0.40}$	$8.533^{+0.045}_{-0.048}$	$9.76^{+0.15}_{-0.16}$
9	90^{+10}_{-10}	$7.752^{+0.106}_{-0.099}$	$9.12^{+0.24}_{-0.18}$	$4.53^{+0.62}_{-0.53}$	$8.605^{+0.102}_{-0.212}$	$9.73^{+0.12}_{-0.10}$
10	50^{+10}_{-10}	$7.581^{+0.095}_{-0.150}$	$9.55^{+0.21}_{-0.25}$	$3.31^{+0.37}_{-0.32}$	$8.507^{+0.075}_{-0.090}$	$9.64^{+0.12}_{-0.12}$

Notes. From left to right, the columns correspond to the GMC number, the instantaneous SFR, the stellar mass ($M_\star$), the characteristic star formation timescale ($\tau_\star$), the stellar metallicity ($Z_\star$), the bolometric luminosity (L_{bol}), and the stellar age; all including 1σ uncertainties. A complete list of results is provided in Table B.1.

Table 6. CIGALE results for star-formation-related properties.

GMC	SFR_{INST} [$\times 10^{-4}\ M_\odot\ yr^{-1}$]	SFR_{100Myr} [$\times 10^{-4}\ M_\odot\ yr^{-1}$]	SFR_{10Myr} [$\times 10^{-4}\ M_\odot\ yr^{-1}$]	$M_\star$ [$\log_{10}(M_\odot)$]	τ_{burst} [$\log_{10}$(yr)]	$M_{\star,old}$ [$\log_{10}(M_\odot)$]	$M_{\star,young}$ [$\log_{10}(M_\odot)$]	Age [$\log_{10}$(yr)]
1	20.76±3.81	23.27±4.43	20.95±3.82	6.70±0.07	8.15±0.33	6.70±0.04	7.87±0.09	9.41±0.57
2	31.02±4.81	26.37±7.53	31.80±4.82	7.17±0.06	8.32±0.31	7.17±0.04	8.10±0.09	9.52±0.93
3	262.01±73.46	292.05±60.68	264.88±75.60	7.82±0.07	8.10±0.33	7.82±0.04	7.74±0.09	9.36±0.55
4	642.50±71.84	446.83±66.94	655.24±73.26	8.50±0.02	8.39±0.33	8.50±0.01	8.16±0.09	9.54±1.03
5	1956.59±262.37	204.02±24.33	2024.70±239.81	8.17±0.02	8.26±0.33	8.17±0.01	7.92±0.09	9.44±0.83
6	476.20±68.99	509.41±79.90	481.12±70.22	7.94±0.06	8.23±0.33	7.94±0.04	7.93±0.09	9.44±1.04
7	191.88±38.04	214.98±40.54	193.54±37.91	7.68±0.06	8.03±0.33	7.68±0.04	7.68±0.09	9.33±0.52
8	47.72±12.44	46.49±10.59	49.32±12.65	7.51±0.07	8.02±0.33	7.51±0.04	7.75±0.09	9.36±0.64
9	35.29±6.93	41.35±8.98	35.72±6.92	7.18±0.06	8.15±0.31	7.18±0.04	7.71±0.09	9.35±0.64
10	32.41±5.98	38.11±9.19	32.98±6.07	7.17±0.07	8.22±0.33	7.17±0.04	7.82±0.09	9.40±0.58

Notes. From left to right, the columns correspond to the GMC number, the instantaneous SFR, the integrated SFR over the last 100 Myr, the SFR over the last 10 Myr, the stellar mass ($M_\star$), the age of the last stellar burst (τ_{burst}), the old stellar population mass ($M_{\star,old}$), the young stellar population mass ($M_{\star,young}$), and the stellar age; all including 1σ uncertainties. Additional results are listed in Tables A.2, A.3, and A.4.

Table 7. Best-fitting results derived for each studied GMC by STARLIGHT.

GMC	adev [%]	$\mathrm{Lum_{tot}}$ [$L_\odot$]	$\log M_\star$ [$M_\odot$]	v_0 [km s^{-1}]	$\sigma_\star$ [km s^{-1}]	A_V	δA_V	$x(\delta A_\mathrm{V} > 0)$ [%]	$\tilde{A}_\mathrm{V}$	$\langle \log t_* \rangle_L$ [yr]	$\langle \log t_* \rangle_M$ [yr]	$\langle \log Z/Z_\odot \rangle_L$	$\langle \log Z/Z_\odot \rangle_M$
1	1.85	9.82	4.94	−2.41	107.86	2.12	3.85	0.00	2.12	8.95	9.79	0.06	0.15
2	2	234.68	5.27	−11.02	113.8	2.22	7.24	2.76	2.42	9.15	8.77	−0.07	−0.07
3	4.3	160.71	6.28	11.63	154.93	4.44	0	23.78	4.44	8.72	9.86	0.02	0.13
4	3.56	6241.17	6.23	1.37	83.82	3.35	5.77	40.23	5.67	7.33	7.22	0.22	0.17
5	3.46	229.04	6.35	−18.47	126.71	4.66	0	4.75	4.66	8.51	9.89	−0.09	0.26
6	3.03	251.04	6.05	−39.4	125.21	3.59	2.04	24.95	4.1	8.66	9.88	−0.11	−0.25
7	2.73	310.66	5.8	−62.53	133.2	1.85	3.94	28.56	2.97	8.57	9.82	0.46	0.54
8	2.77	40.41	5.63	−59.2	106.07	2.28	4.46	0.00	2.28	9.69	9.95	−0.4	−0.51
9	2.65	22.74	5.35	−56.9	116.32	1.84	4.22	0.00	1.84	9.57	9.78	−0.12	−0.18
10	2.14	74.93	5.01	−69.57	124.54	1.43	3.61	18.89	2.12	8.6	9.08	0.55	0.55

GMC	$(F_{H\alpha}/F_{H\beta})_{obs}$	A_V^{Balmer} [mag]	A_V^{CIGALE} [mag]	$\tilde{A}_V^{STARLIGHT}$ [mag]
1	3.81 ± 0.32	1.08 ± 0.11	3.57 ± 0.02	2.12
2	8.32 ± 1.70	2.89 ± 0.30	3.58 ± 0.02	2.42
3	29.79 ± 16.90	5.06 ± 0.56	6.04 ± 0.11	4.44
4	45.69 ± 37.94	5.87 ± 0.67	6.06 ± 0.00	5.67
5	43.43 ± 37.37	5.81 ± 0.65	6.24 ± 0.02	4.66
6	29.14 ± 16.45	5.04 ± 0.54	6.08 ± 0.01	4.10
7	21.21 ± 10.11	4.38 ± 0.47	5.07 ± 0.02	2.97
8	19.18 ± 10.04	4.18 ± 0.45	3.53 ± 0.01	2.28
9	17.01 ± 7.84	3.96 ± 0.42	3.54 ± 0.01	1.84
10	11.13 ± 5.05	3.36 ± 0.37	3.54 ± 0.12	2.11

Notes. Attenuation estimates for the studied GMCs derived from the Balmer decrement (A_V^{Balmer}), CIGALE (A_V^{CIGALE}), and effective A_V ($\tilde{A}_V^{STARLIGHT}$) from STARLIGHT. The first two columns correspond to the GMC number and the Hα over Hβ observed flux ratio, from left to right, respectively.